AN INVESTIGATION OF CORNER SEPARATION WITHIN A THRUST AUGMENTER HAVING COANDA JETS*

M. R. Seiler

Rockwell International
Columbus Aircraft Division

- Abstract -

An investigation was conducted to determine the way separation develops in the corners of thrust augmenter wings having Coanda jets. Hot film surface sensors and pressure transducers were used, and the results indicated that separation on the test augmenter began at a corner very close to the augmenter exit and then rapidly proceeded upstream. Measurements of the pressure fields in the corner region indicated that a modified form of the Stratford criterion could be used to predict the onset of separation. Testing was conducted over a range of nozzle pressure ratios, aspect ratios, diffuser angles and designs of the boundary layer and Coanda nozzles.

*Research supported by the Naval Air Development Center, Contract N62269-76-C-0402, Final Report No. NADC 76153-30

I. Introduction

Thrust augmenters have been used in aircraft applications for a number of years. One of the first applications was to use them to draw cooling air over a jet engine nozzle.[1] Modest increases in thrust were also observed. During the early 1960's thrust augmenters were used to provide lift for the XV-4A research VTOL aircraft. More recently[2] they have been used in the design concept of thrust augmenter wings (TAW) for direct lift in the Navy XFV-12A. Experimentally it has been observed that flow separation within the augmenter diffuser is often the limiting factor. The purpose of this study was to conduct a suitable testing program and analysis of an unswept, untapered (rectangular), model augmenter so that a preliminary separation criterion could be established.

II. Approach

The type of augmenter under consideration is one having a centerjet and two Coanda jets, as shown in Figure 1. The Coanda jets originate upstream of the throat and provide a wall jet through the diffuser section. Without these Coanda jets, diffuser half-angles are limited to $\delta_D \approx .1$ radian to prevent separation. Small, boundary layer control (BLC) blowers were also mounted through the endwall and could be rotated manually to direct flow parallel to the diffuser flap. The end elements of the cross-slot centerbody also direct some flow onto the endwalls to accomplish a BLC function. Figure 2 shows a photograph of the test augmenter looking into the exit.

Flow to each of the major augmenter components was measured by a separate venturi and nozzle pressures were recorded by a total pressure probe at the nozzle exit. Nozzle pressure ratios were varied between 1.5 and 2.5. The entire 50 cm (20") span augmenter was mounted on a horizontal cradle suspended by four tie-rods attached to a rigid frame. Two 500-pound load cells measured the thrust. The tares of the flexible hoses, which deliver the primary air, were recorded versus supply pressure and removed from the measured thrust. A 4500 hp Ingersoll-Rand compressor was used as the continuous air supply.

Experience has shown that flow separation generally occurs at or near a corner formed by the diffuser and the endwall.[3] There are two possible modes through which separation might develop (Figure 3). In the first mode separation would initiate at the augmenter exit and, because of the adverse pressure gradient within the diffuser, rapidly progress upstream. A second possible mode would be for separation to begin in the corner on the highly stressed Coanda surface and then proceed downstream until the entire diffuser corner was involved.

The type of BLC being used may have an effect on the separation mode and the angle at which separation occurs. The aspect ratio (AR = span/throat

width) also effects the separation angle.[4] Finally, a reasonable data base should include testing over a wide nozzle pressure range.

The objective of the study was then to accomplish the following tasks:

a) To determine which of the two possible corner separation modes actually occur in an operating augmenter with Coanda jets.

b) To measure the pressure and velocity fields in the vicinity of the separation point for a range of nozzle pressure ratios (P_R) and BLC conditions at and near separated flow conditions.

c) To alter the augmenter AR and repeat task b, above.

d) To alter the Coanda design to provide comparative data on Coandas of smaller R/t. This provides a more highly stressed Coanda surface. In addition, the internal Coanda nozzle configurations were altered to examine the possible effects of exit velocity profile on separation.

e) To analyze the data to derive a separation criteria.

III. Results

For all tests the throat width, flap length, centerbody and BLC were as shown in Figure 1. Three different Coanda configurations, shown in Figure 4, were used. The first, called a reference profile, maintained a Coanda radius to nozzle gap ratio of 26.5. The ratio of augmenter throat area to total nozzle area was $A_2/A_0 = 20.5$. This reference Coanda was used in the study of separation mode and to provide a baseline augmentation ratio versus diffusion ratio, A_3/A_2.

Separation Mode

The augmenter was instrumented as shown in Figure 5. Two flush-mounted Thermo-Systems, Inc., Model 1237 hot film sensors were mounted on one flap surface at the endwall corner .032 cm and 5.01 cm upstream from the flap trailing edge. Two Statham ±2 psi differential pressure transducers were connected to surface pressure taps similarly located on the opposite flap. The hot film sensors were connected to a model 1050-2C Thermo-Systems, Inc., dual channel constant temperature anemometer whose output, together with that of the two transducers, was connected to a multi-channel Consolidated Electronics Corporation oscillograph.

The response time of the hot-film sensor ($\approx 5 \times 10^{-6}$ sec) was an order of magnitude faster than any mean flow changes likely to occur within the augmenter. Using the A.C. anemometer output, the diffuser angle, θ_D, was gradually increased to a point where a slight buffeting could be

detected audibly (incipient separation). As shown in Figure 6 the turbulence level increased suddenly at the downstream sensor. Next the augmenter δp was rapidly raised beyond the point of attached flow and the two signals were displayed on the oscilliscope. Turbulence levels on the upstream sensor increased markedly within .0023 to .0027 seconds after the downstream sensor showed a similar increase. These tests, done at a nozzle pressure ratio of 2.0, show that the separation was initiating downstream. Similar results were obtained at a pressure ratio of 1.5.

Augmentation Ratio

The augmentation ratio is defined:

$$\emptyset = \frac{\text{measured load-stand thrust}}{\text{ideal thrust from all primary jets and BLC}}$$

where the ideal thrust uses the measured venturi mass flow and the isentropic nozzle velocity (expanded to atmospheric pressure). Using the reference profile Coandas, the results of Figure 7 were obtained with aspect ratio = 4.1. Notice that separation occurs at a half angle of .21 radian without BLC and at .35 radian with BLC. When the aspect ratio is changed to 2.5, Figure 8 shows that the overall $\emptyset$ levels are similar but separation occurs at a slightly lower diffuser angle. A_2/A_0 was 20.5. BLC blowers were manually adjusted to blow parallel to the flaps.

Subsequent tests at A_2/A_0 = 17 were made on the top-hat profile and the vortex profile Coandas of Figure 4. The top-hat was designed to achieve a uniform velocity profile at the nozzle but R/t was reduced to 9.3. The vortex profile Coanda was intended to produce a nozzle velocity that was greatest on the inner radius.

Figure 9 shows results of augmentation ratio versus A_3/A_2 for the top-hat profile. Although the initial slope, $\emptyset$ vs A_3/A_2, is similar to the reference profile, flow separation in the diffuser corner limits the performance to lower values of $\emptyset$.

Similar behavior was also noted on the vortex profile Coanda (Figure 10). At nozzle pressure ratios of 2.5, corners became more difficult to attach on both of these Coanda shapes.

Pressure Measurements

A series of 13 flush-mounted static taps were added in one corner of the diffuser near the exit, as shown in Figure 11. These taps were connected to a water manometer and recorded during operation at all diffuser angles. Also recorded was the throat secondary static pressure. Figure 12 shows the location of the probe.

Figures 13 and 14 show the static pressure profiles in the diffuser corner for the reference profile Coanda. These measurements were taken at the diffuser angle for incipient separation, which also corresponds to the angle for maximum $\emptyset$. Figure 13 gives results without BLC for an aspect ratio of 4.1. Figure 14 is for full BLC; that is, the BLC nozzle pressure was set equal to the Coanda and centerjet pressures. Also shown in the figures are the calculated term xdp/dx exit, which is derived from the gradient of the pressure readings. The trend is toward a steeper gradient at the diffuser exit as the BLC is applied. Nominal A_2/A_0 was 20.5.

Figures 15 and 16 show results for the top-hat and vortex profile Coandas at an aspect ratio of 4.1. A_2/A_0 was 17. Notice that the static pressures are more negative than for the reference profile and the gradient is more steep. This is related to the increased Coanda nozzle gap and the reduced A_2/A_0.

IV. Separation Criteria

One of the more successful airfoil separation criteria and the one considered herein is that of Stratford[5] where the criteria is expressed as a non-dimensional number N_{ST},

$$N_{ST} = \frac{C_P \ (xdC_P/dx)^{1/2}}{(R_N \times 10^{-6})^{1/10}} \qquad (1)$$

where Cp is the pressure coefficient, defined by

$$C_P = \frac{P(x) - P(0)}{q(0)} \qquad (2)$$

Cp is based upon the difference between local wall static pressure P(x) and that pressure occurring at the start of the interaction region, P(0), at x = 0. q(0) is the dynamic pressure $1/2\rho U_{max}^2$, where U_{max} is the maximum velocity at x = 0. R_N is the Reynolds number based upon U_{max} and x. Stratford's method involves an approximate solution of the equations of motion, and matching the solutions at the junction of the "inner" and "outer" boundary layer. A subsonic airfoil will not separate if $N_{ST} < .37$.

Although Stratford used P(0) as the wall pressure at x = 0, there are experimental difficulties in determining its value accurately on a Coanda radius at choked pressures. Furthermore, because of the highly curved flow near the Coanda, the value of P(0) at the wall is also difficult to predict analytically. For these reasons, P(0) was chosen for the ejector diffuser to be the value of the static pressure in the uniform secondary stream (see Figures 12 and 17).

$q(0)$ is merely a normalizing factor for the other pressure terms. Rather than take $q(0) = 1/2\rho U_{max}^2$ at the throat, it seemed correct in the high Mach number flow to use $q(0)$ as the maximum gage total pressure. Experience has shown that all static pressures (gage) in an augmenter can be normalized by nozzle gage total pressure. In a corner near the throat, the maximum value of q is either:

(1) The gage total pressure set on the BLC blower, or

(2) The gage total pressure of the Coanda flow.

The greater of the above two quantities was used to set $q(0)$. With no BLC turned on, the Coanda flow sets $q(0)$. With full BLC, the BLC nozzle pressure determines $q(0)$. Since R_N must use the maximum velocity U_{max}, the isentropic flow equations were used to determine the relationship between U_{max} and $q(0)$ (see Figure 18).

$$U_{max} = \left(2RT \frac{\gamma}{\gamma-1} \left(1 - P_R^{-\frac{\gamma-1}{\gamma}}\right)\right)^{1/2} \text{ meters/sec} \qquad (3)$$

R = 287 Joules/°K-kg
γ = 1.4
T = temperature, °K (nominally 290°K)
P_R = $(q(0) + P_\infty)/P_\infty$
P_∞ = barometric pressure (nominally 99 Kilopascals)

Table I presents a summary of the Stratford number calculations for the augmenters constructed under the present study. There are three BLC conditions--full, minimum and no BLC for aspect ratios of 4.1 and 2.5 using the reference Coandas. Also included are the top-hat and vortex profile Coanda results. The table gives the nominal pressure ratio and the flap angle where the measurements and calculations were made.

It is instructive to consider the difference in the three augmenters and to try to visualize what mechanism is setting $N_{ST} = .02$ as a common upper limit. Figure 19 shows a plot of the term $P_\infty - P(0) = P(x) - P(0)$ and the term xdP/dx versus diffuser angle for the three augmenters. The conditions are full BLC and PR = 2.0. Notice that the vortex and top-hat profiles produce larger values of xdP/dx than does the reference profile. This, as mentioned earlier, is related to the larger nozzle gap and decreased A_2/A_0. The throat static gage pressure, or its negative, $P_\infty - P(0)$, is also greater for the vortex and top-hat at small diffuser angles. This is due to the reduced overall A_2/A_0. Finally near .175 to .2 radian, the reference profile produces the largest values of xdP/dx and $P_\infty - P(0)$. The reference profile also produces the greatest $\emptyset$.

A lesson to be learned from Figure 19 is that a high $\emptyset$ augmenter should produce a large drop in throat static pressure (as is well known) but simultaneously must not produce a large value of xdP/dx at the exit.

This implies that small primary nozzles should be used to achieve well-mixed flows and nearly ambient static pressures at the exit. In other words, the exit static pressure should be nearly recovered to ambient. These facts are entirely consistent with the experience of many workers in the area of thrust augmentation.

Figure 20 shows the calculated values of N_{ST} for these augmenters under the same operating conditions; i.e., full BLC and PR = 2.0. The Stratford number rises to a maximum as flap angle is increased and does provide a useful separation criteria.

These plots indicate that we have not mistakenly selected a criteria this is insensitive to flap angle. The flow will be stable and attached provided

$$N_{ST} \leq .0196$$

For flap angles that produce separation, the Stratford number has no meaning; that is, the criteria is to be used only in the range of flap angles where $d N_{ST}/d\delta$ is positive.

It should be noted that some care in selecting BLC orientation is needed if these experiments are to be repeated. As stated earlier the BLC tubes were rotated manually to direct flow parallel to the flap. If this is not done, the unusual exit pressure profiles of Figure 21 will be obtained. Case 1 is caused by directing the BLC flow into the flap. It likely represents a helical flow pattern in the corner. Case 2 is similar with the opposite flap attached. Case 3 is the profile most like those of this study, with BLC blowing parallel to the flap. Case 4 is a separated flap.

V. Conclusions

1. Corner separation of the test thrust augmenting wing-type augmenter initiates at or near the augmenter diffuser exit and then rapidly progresses upstream until the whole corner from the vicinity of the augmenter throat to the exit is involved.

2. A modified form of the Stratford airfoil stall criterion successfully correlates the onset of augmenter separation in the test augmenter where the independent test variables were nozzle pressure ratio, augmenter aspect ratio, boundary layer control blower pressure ratio and Coanda configuration. The modification consists of a change in reference pressure, P(0), and in definition of q.

3. Circular Coandas with small R/t cause separation to occur at lower diffuser angles.

References

1. Greathouse, W. K., "Preliminary Investigation of Pumping and Thrust Characteristics of Full-size Cooling Air Ejectors at Several Exhaust-Gas Temperatures," NACA RM E54A18, 1954.

2. Throndson, L. W., "Compound Ejector Thrust Augmentation Development," ASME 73-GT-67, 1973.

3. "Three-Dimensional Effects on Augmenters," Rockwell International Report NR76H-36, 1976.

4. Stewart, V. R., "A Study of Scale Effects on Thrust Augmenting Ejectors," Rockwell International Report NR76H-2, 1976.

5. Stratford, D. S., "The Predictions of Separation of the Turbulent Boundary Layer," J. Fluid Mechanics, p. 1, January 1959.

TABLE I.

SUMMARY OF STRATFORD NUMBER CALCULATIONS

Case	Nom. Pressure Ratio	Flap Angle, Radians	P(x) Pascals (Gage)	P(o) Kilo-pascals (Gage)	Q(o) Kilo-pascals	[xdP/dx] exit Kilopascals	$R_N \times 10^{-6}$	N_{ST}*	Remarks
Reference Profile	1.5	0.33	−200	− 6.0	51.0	2.32	2.99	0.0217	Q(0) set by BLC
1. R/t = 26.5	2.0	0.33	−400	−11.5	102.0	4.60	3.81	0.0202	nozzle pressure
Full BLC, AR = 4.1	2.5	0.33	−650	−15.0	147.0	6.95	4.25	0.0184	which is identical to all other nozzles.
Reference Profile	1.5	0.33	−200	− 5.0	47.4	2.32	2.92	0.0201	Q(0) set by BLC
2. R/t = 26.5	2.0	0.33	−450	− 9.7	91.5	4.65	3.68	0.0200	nozzle pressure.
Min. BLC, AR = 4.1	2.5	0.33	−600	−14.0	136.0	6.50	4.17	0.0187	
Reference Profile	1.5	0.21	−150	− 4.2	35.2	1.86	2.58	0.0241	Q(0) set by Coanda
3. R/t = 26.5	2.0	0.21	−375	− 8.1	70.5	3.95	3.28	0.0230	flow at throat.
No BLC, AR = 4.1	2.5	0.21	−550	−11.5	101.0	5.60	3.56	0.0225	
Reference Profile	1.5	0.30	−150	− 5.1	51.0	2.89	2.99	0.0207	Q(0) set by BLC noz-
4. R/t = 26.5	2.0	0.30	−300	− 9.4	102.0	5.12	3.81	0.0175	zle pressure which
Full BLC, AR = 2.5	2.5	0.30	−375	−13.2	147.0	6.85	4.25	0.0163	is identical to all other nozzles.
Reference Profile	1.5	0.30	−125	− 4.85	48.0	3.02	2.92	0.0222	Q(0) set by BLC
5. R/t = 26.5	2.0	0.30	−250	− 9.0	88.0	5.33	3.63	0.0215	nozzle pressure.
Min. BLC, AR = 2.5	2.5	0.30	−375	−12.7	135.0	7.0	4.17	0.0180	
Reference Profile	1.5	0.175	−125	− 3.66	38.0	2.19	2.65	0.0203	Q(0) set by Coanda
6. R/t = 26.5	2.0	0.175	−200	− 6.92	76.0	4.4	3.22	0.0189	flow at throat.
No BLC, AR = 2.5	2.5	0.175	−250	− 9.2	109.0	6.05	3.56	0.0170	
Top Hat Profile	1.5	0.175	−250	− 4.73	51.0	2.44	2.99	0.0172	Q(0) set by BLC noz-
7. R/t = 9.3	2.0	0.175	−450	− 8.7	98.0	6.5	3.77	0.0190	zle pressure which
Full BLC, AR = 4.1	2.5	0.14	−700	−12.3	145.0	9.75	4.24	0.0180	is identical to all other nozzles.
Vortex Profile	1.5	0.175	−225	− 4.93	51.0	3.48	2.99	0.0216	Q(0) set by BLC noz-
8. R/t = 9.3	2.06	0.175	−520	− 9.25	108.0	7.0	3.90	0.0180	zle pressure which
Full BLC, AR = 4.1	2.5	0.14	−575	−11.2	145.0	8.85	4.24	0.0157	is identical to all other nozzles.

$$*N_{ST} = \frac{P(x) - P(0)}{Q(0)} \left[\frac{xdP/dx}{Q(0)}\right]^{1/2} (R_N \times 10^{-6})^{-0.1}$$

Average N_{ST} = 0.0196

Standard Deviation = 0.002 (11%).

CAD 8989

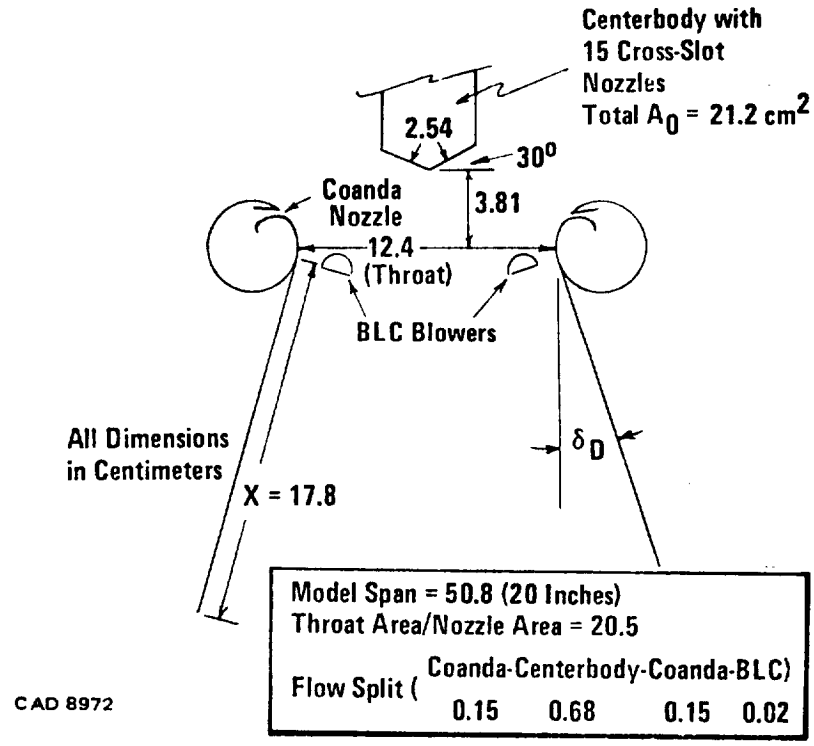

Figure 1. Sectional view of test augmenter.

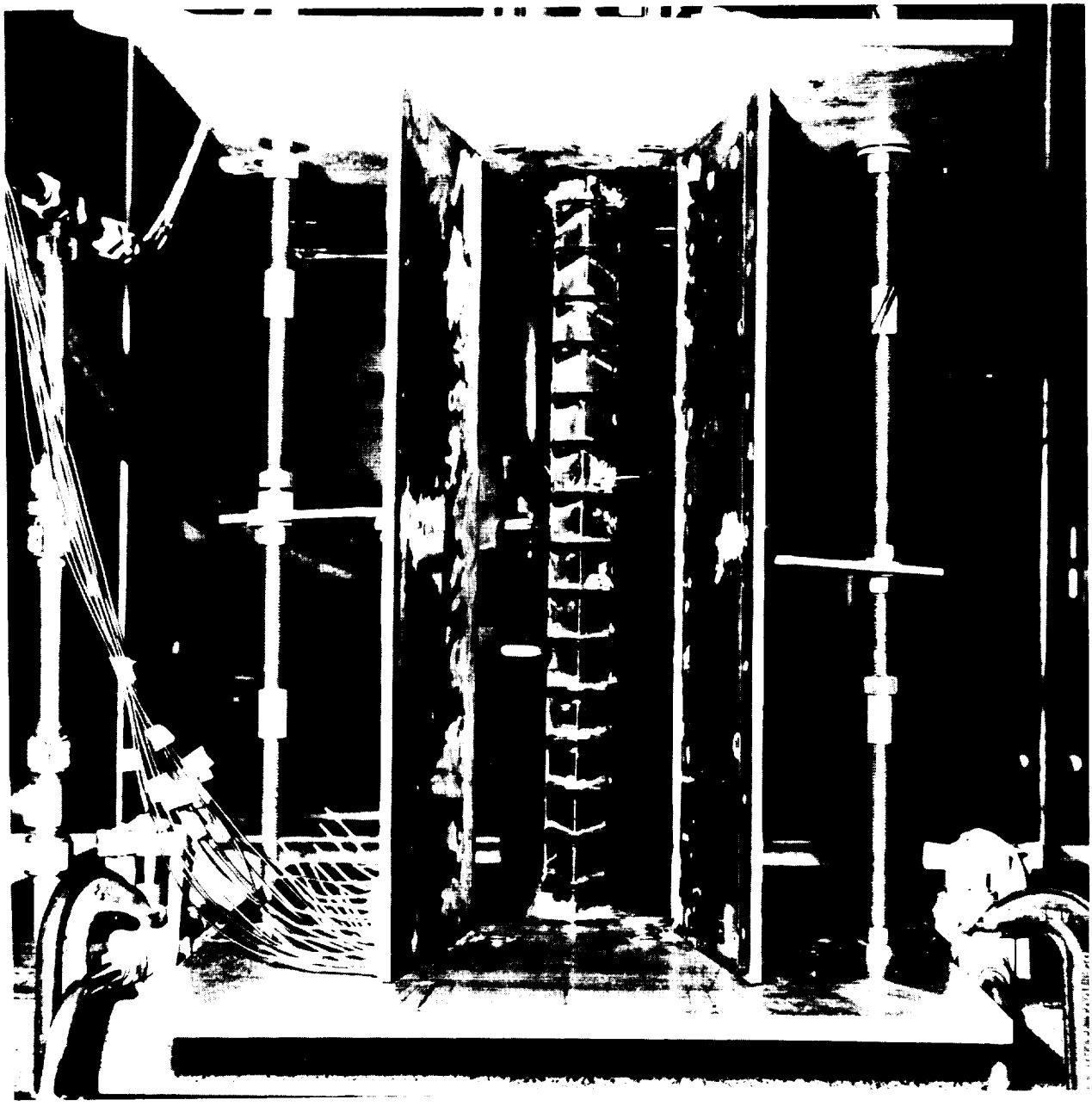

Figure 2. Test augmenter.

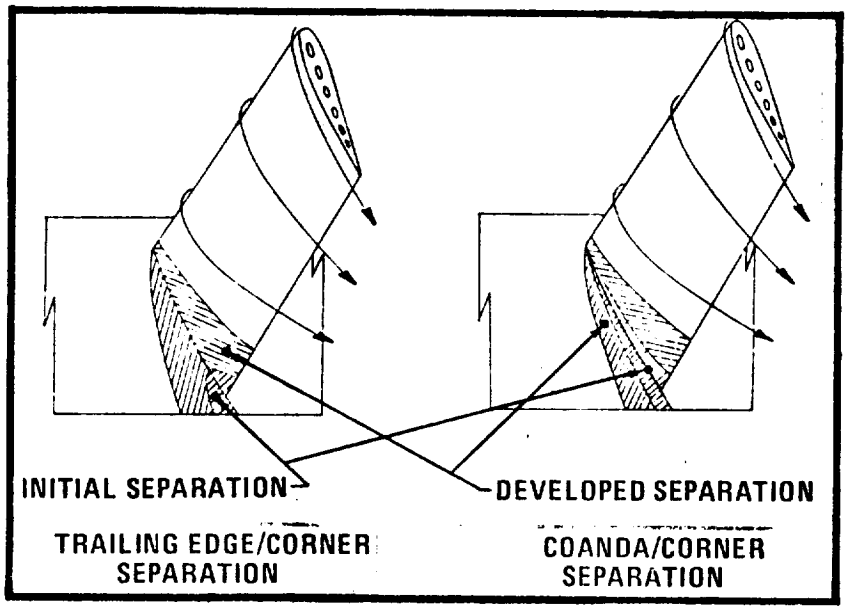

Figure 3.- Possible modes of Corner separation.

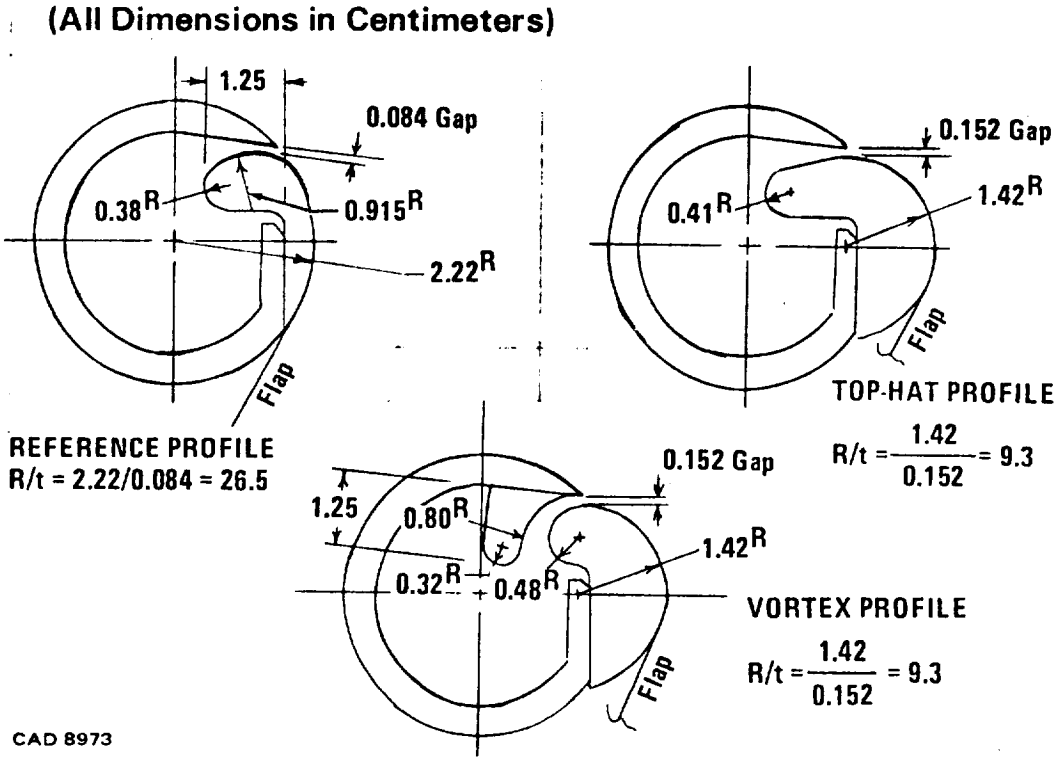

Figure 4. Coanda nozzles tested in present study.

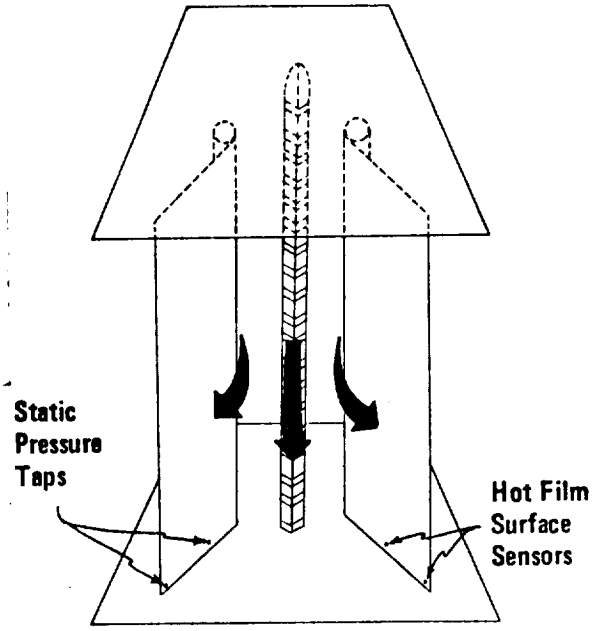

CAD 8976

Figure 5. Instrumentation for separation mode determination.

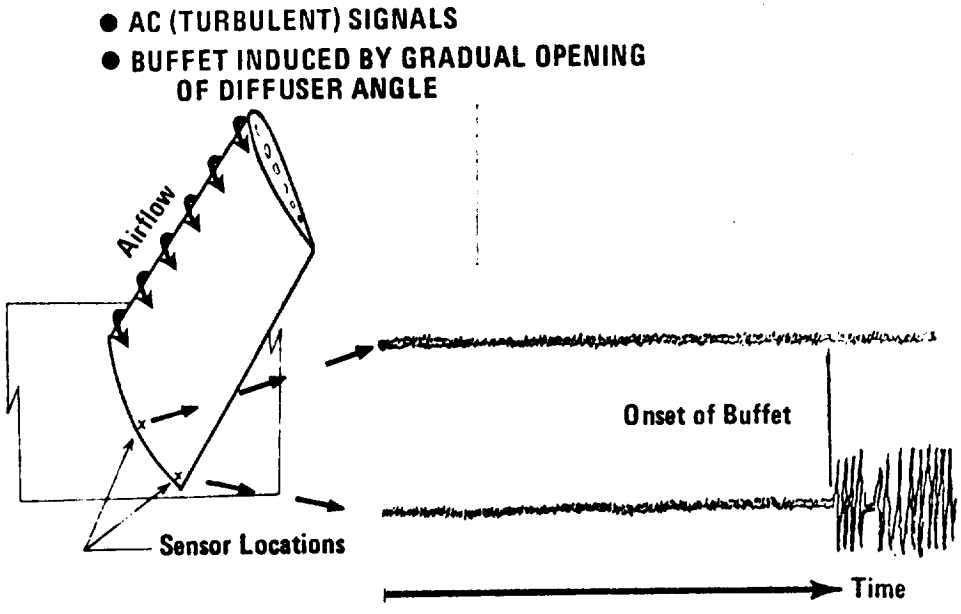

CAD 8977

Figure 6. Buffet response of hot film sensors: $P_R = 2.0$.

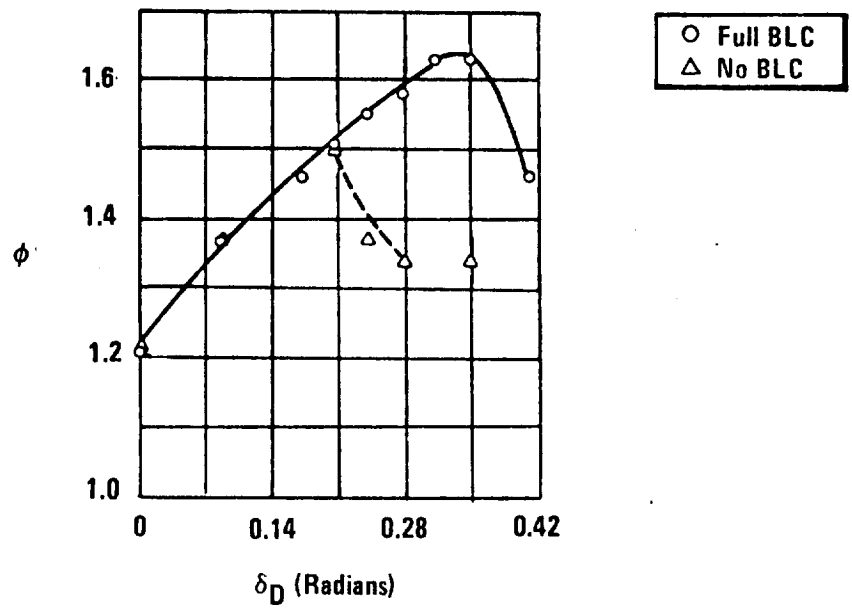

Figure 7. Augmentation ratio vs diffuser angle: AR = 4.1.

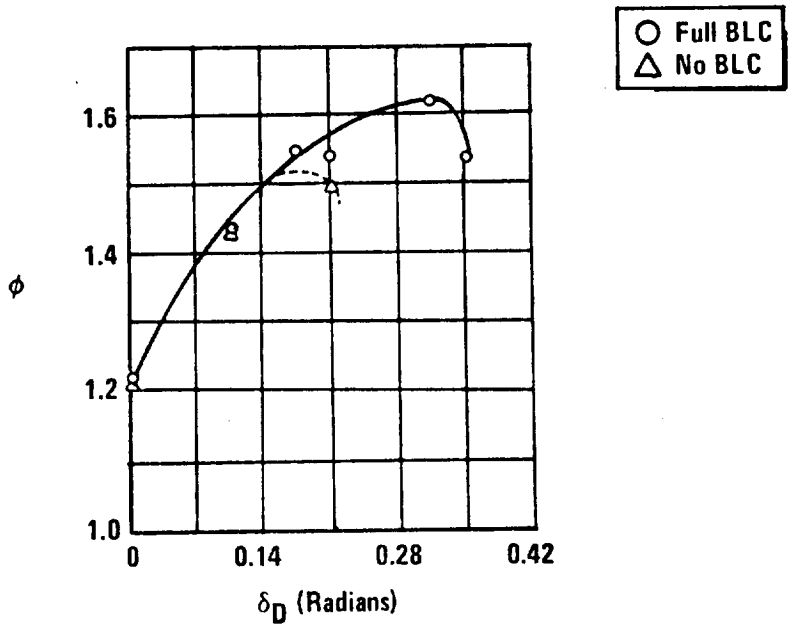

CAD 8975

Figure 8. Augmentation ratio vs diffuser angle: AR = 2.5.

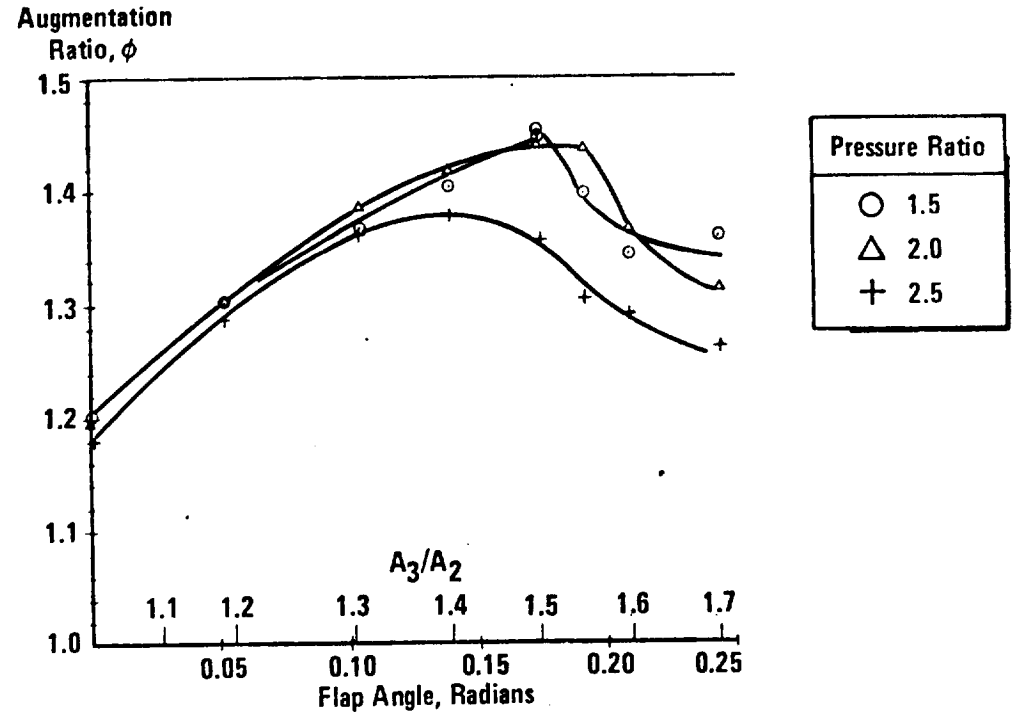

Figure 9. Augmentation ratio vs diffuser angle, top-hat profile.

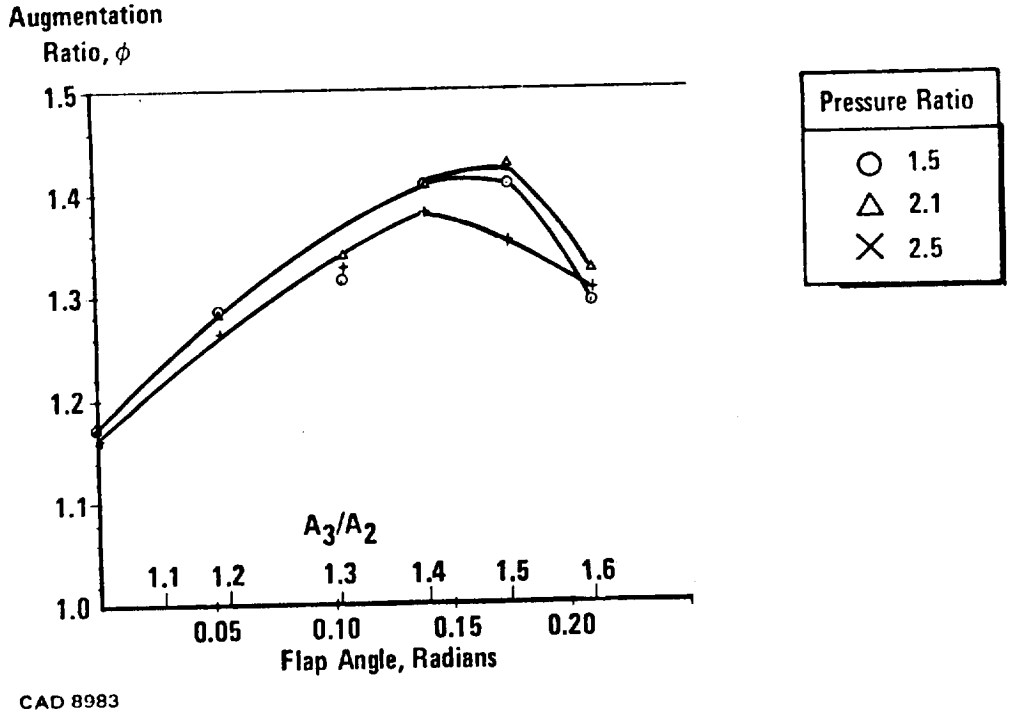

Figure 10. Augmentation ratio vs diffuser angle, vortex profile.

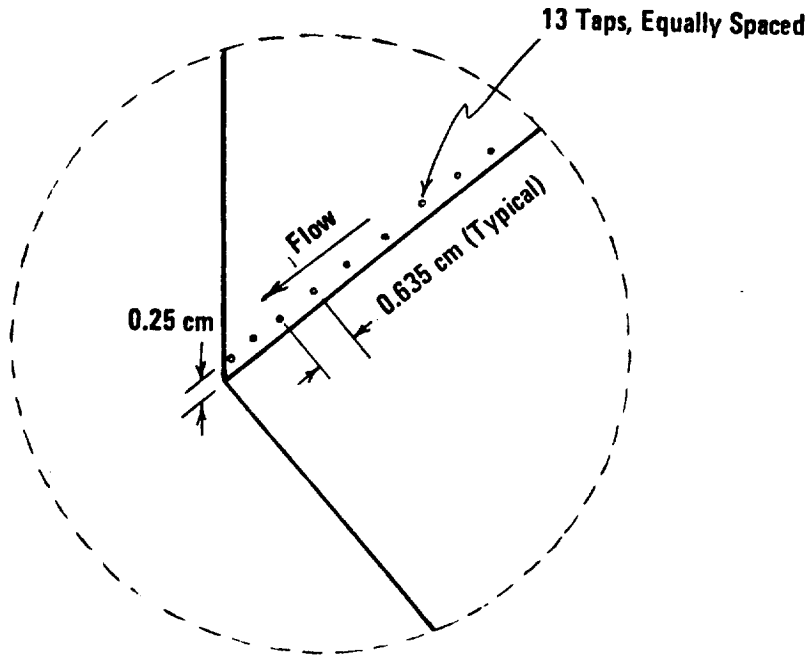

Figure 11. Location of corner static pressure taps.

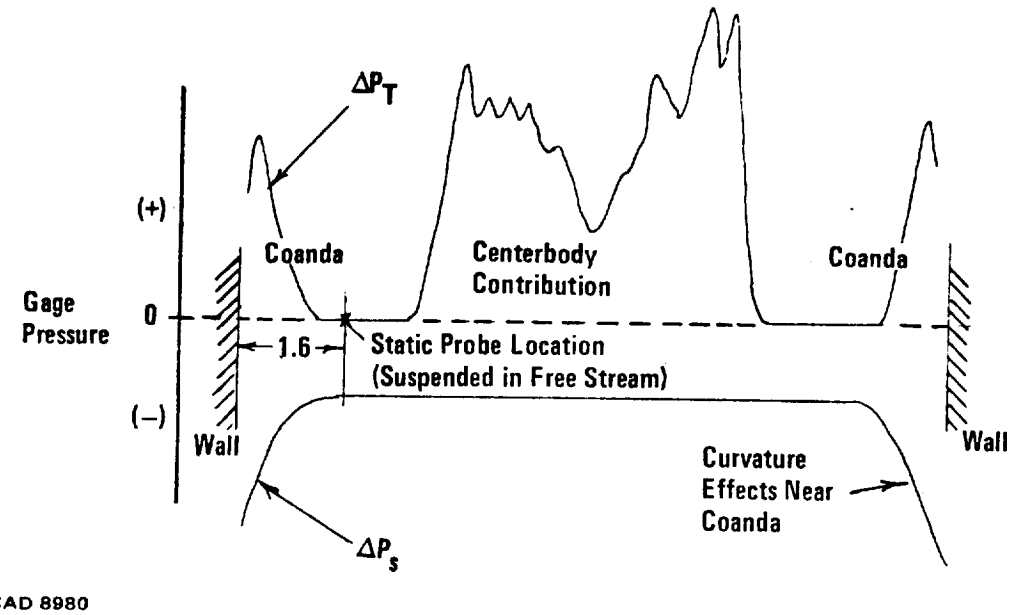

Figure 12. Typical total, ΔP_T, and static ΔP_S distribution across the augmenter throat.

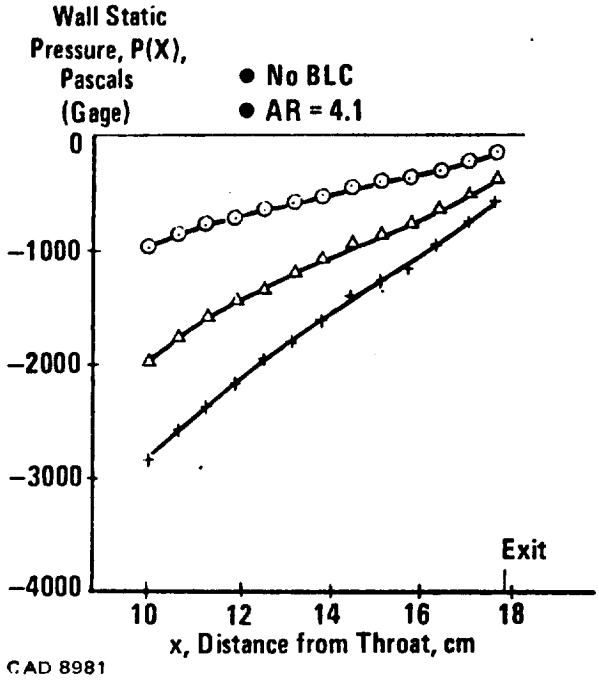

Symbol	Pressure Ratio	Flap Angle Radians	[xdP/dx] exit Pascals
o	1.5	0.21	1860
Δ	2.0	0.21	3950
+	2.5	0.21	5600

Figure 13. Corner static pressure readings for reference profile Coandas, R/t = 26.5, no BLC.

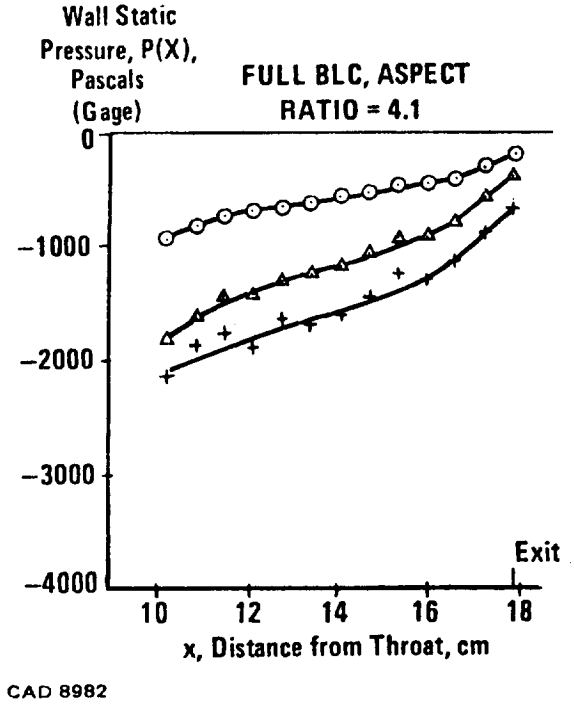

Symbol	Pressure Ratio	Flap Angle Radians	[xdP/dx] exit Pascals
o	1.5	0.33	2320
Δ	2.0	0.33	4600
+	2.5	0.33	6950

Figure 14. Corner static pressure readings for reference profile Coandas, R/t = 26.5, full BLC.

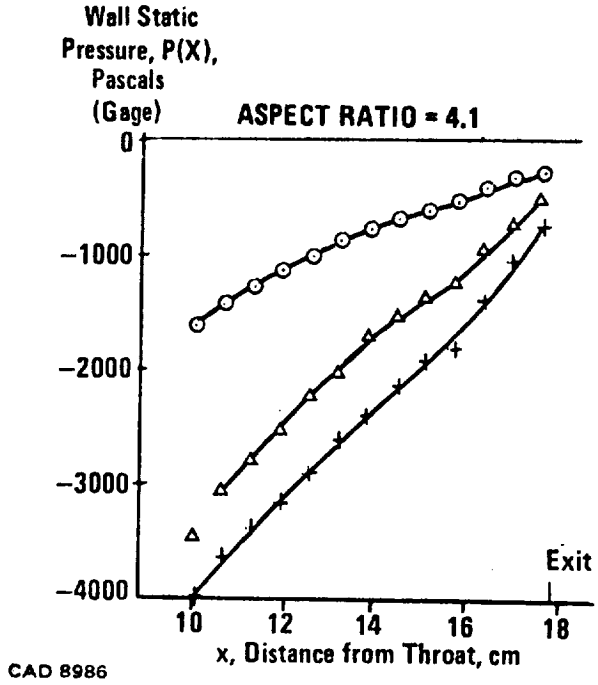

Symbol	Pressure Ratio	Flap Angle Radians	$[xdP/dx]_{exit}$ Pascals
○	1.5	0.175	2440
△	2.0	0.175	6500
+	2.5	0.140	9750

Figure 15. Corner static pressure readings for top-hat profile, R/t = 9.3, full BLC.

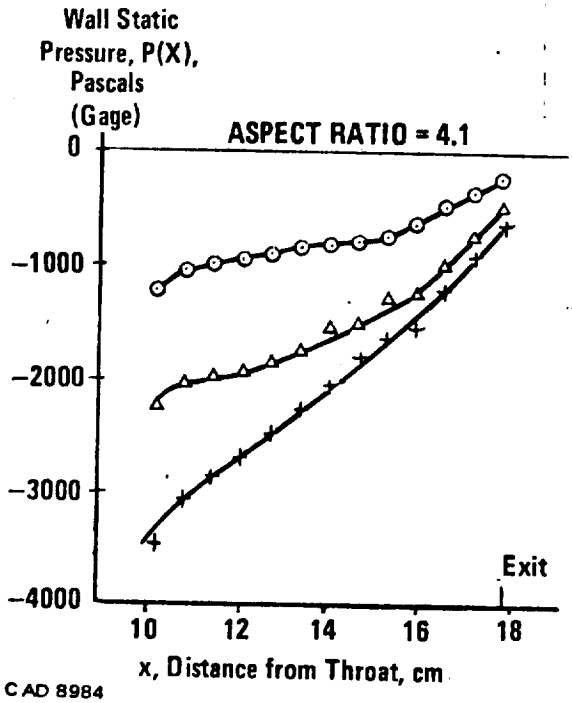

Symbol	Pressure Ratio	Flap Angle Radians	$[xdP/dx]_{exit}$ Pascals
○	1.5	0.175	3480
△	2.1	0.175	7000
+	2.5	0.140	8850

Figure 16. Corner static pressure readings for vortex profile, R/t = 9.3, full BLC.

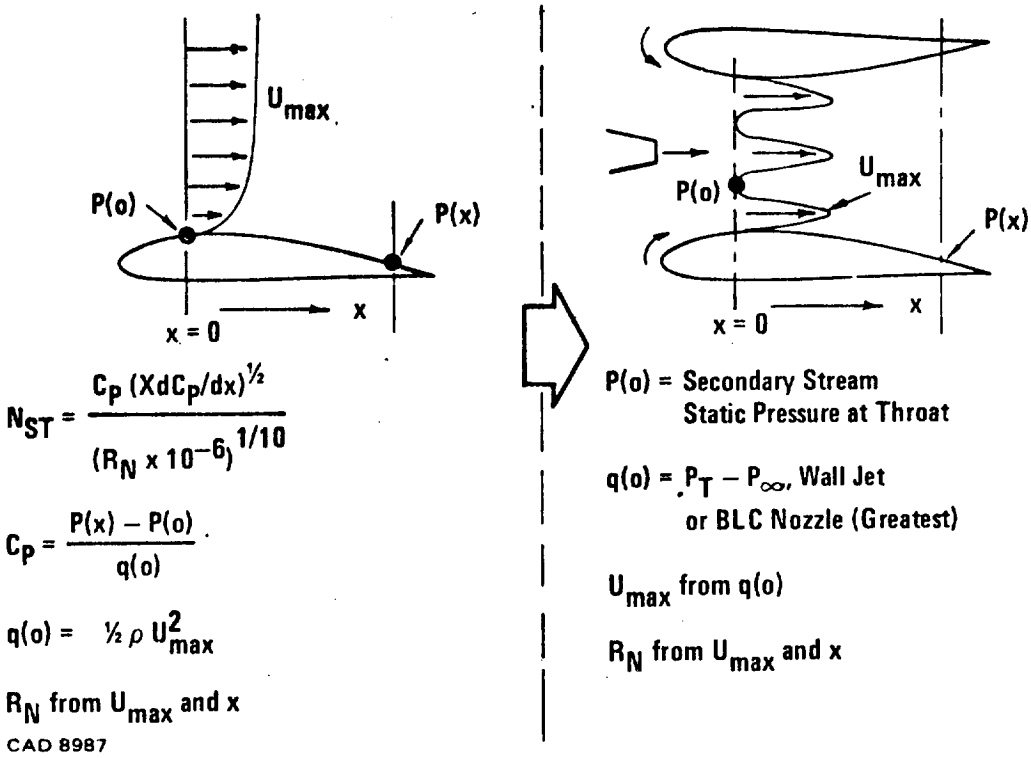

Figure 17. Stratford and modified Stratford.

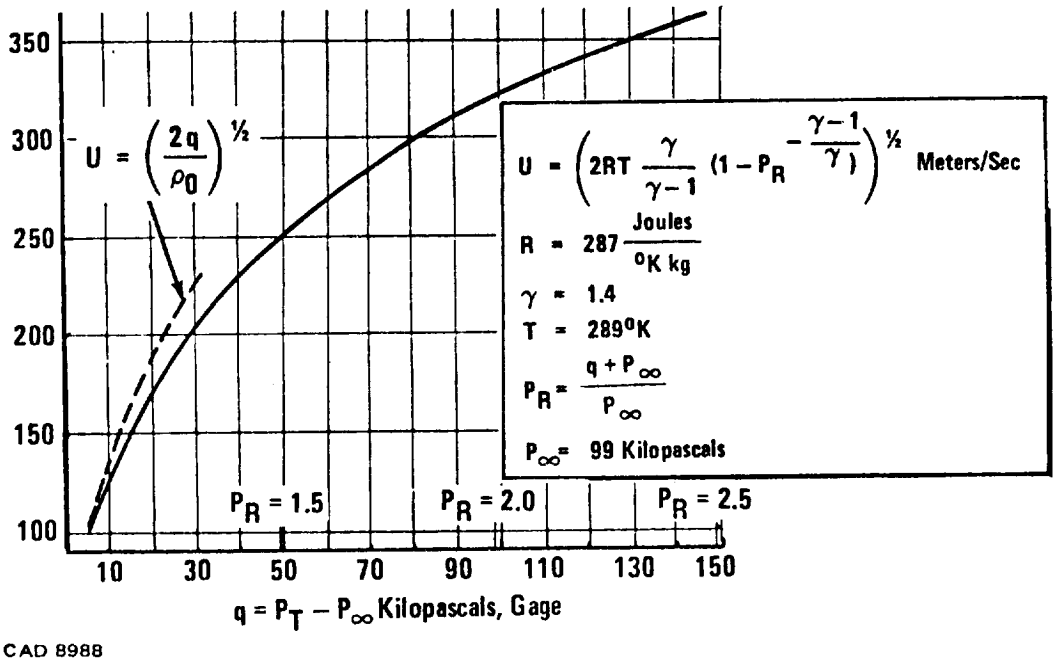

Figure 18. Velocity vs q.

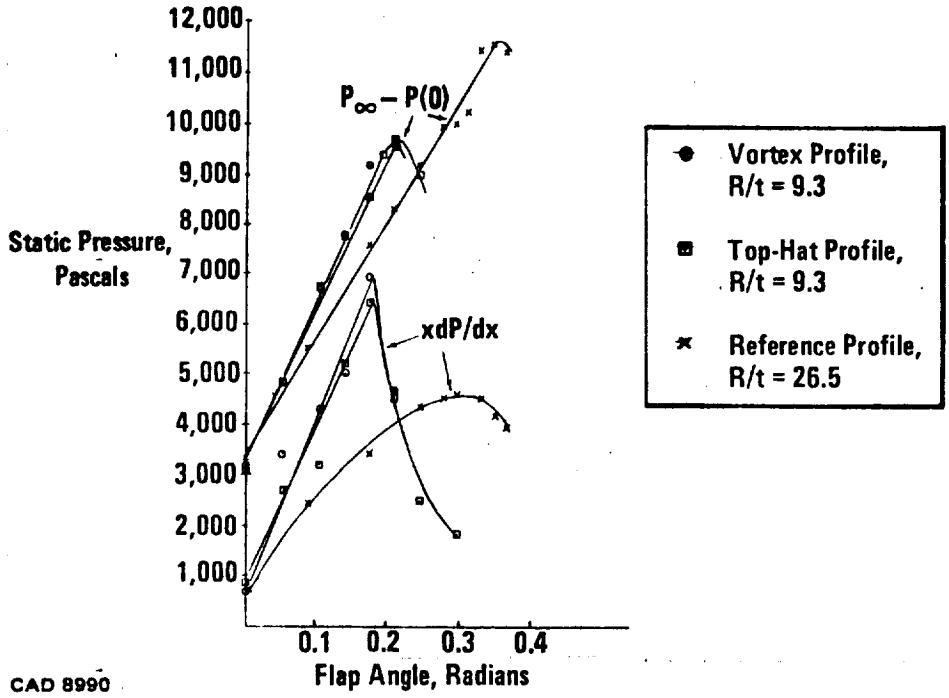

Figure 19. Variation of static pressure components with flap angle.

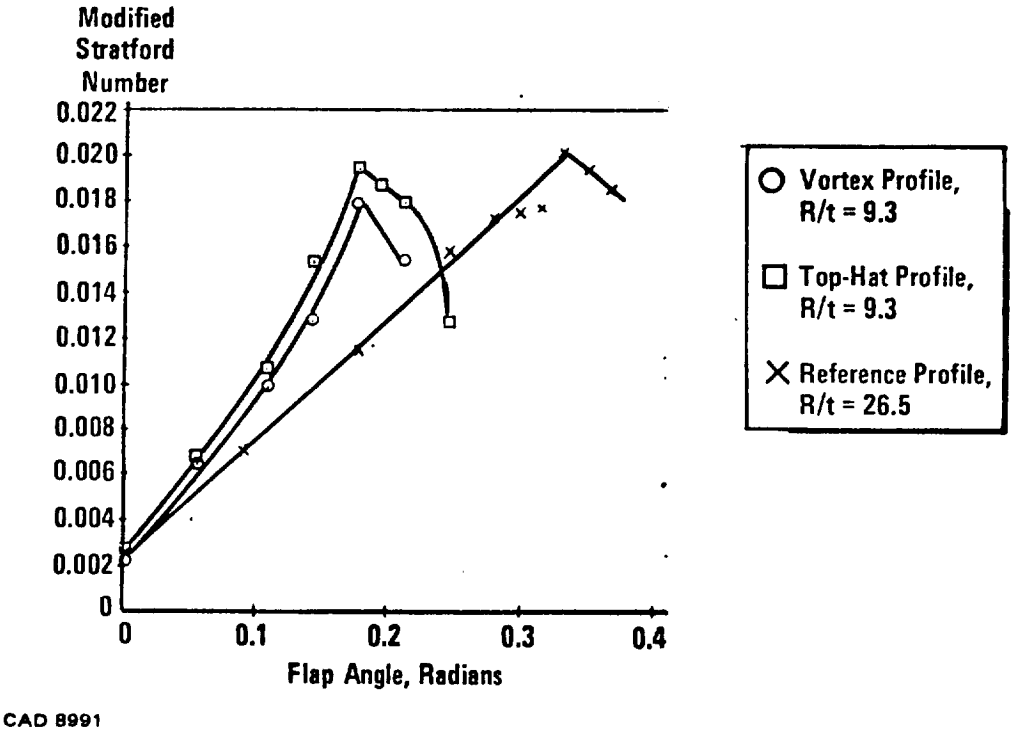

Figure 20. Variation of Stratford number with flap angle.

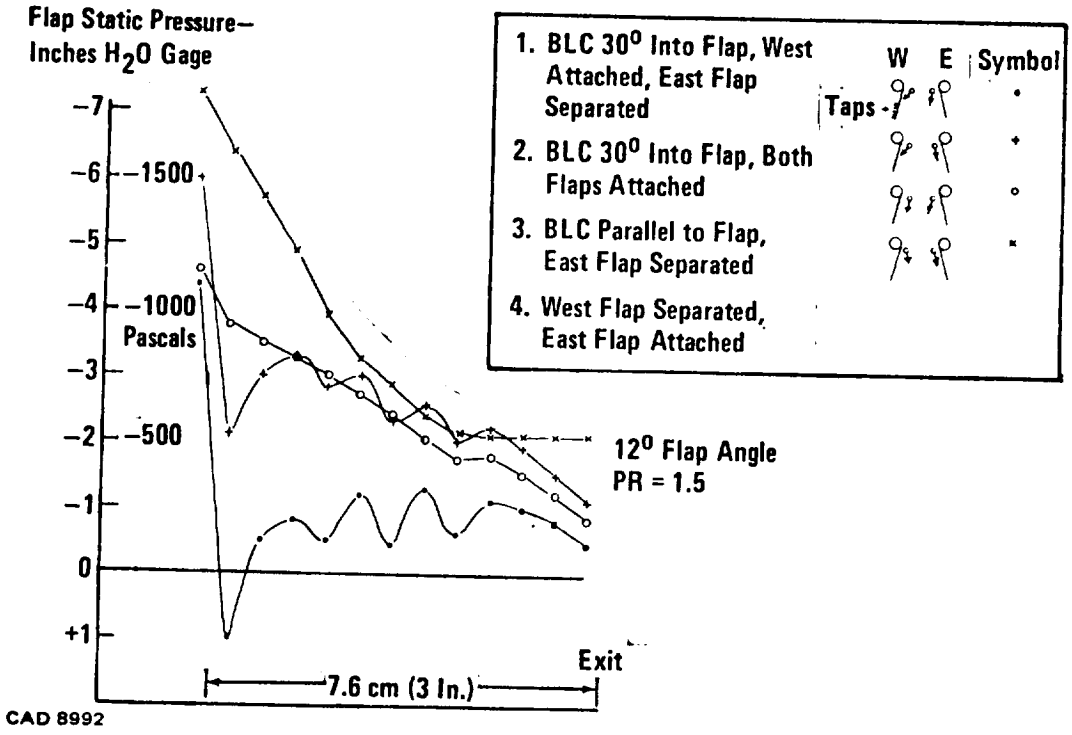

Figure 21. Effects of BLC nozzle orientation on flap statics.